PACS numbers: 42.62.Fi; 78.47.+p; 74.25.Gz; 78.20.Bh
DOI: 10.1070/QE2005v035n08ABEH008973

Degeneracy of electronic states and the 'anomalous' kinetics of a nonlinear response of high-temperature superconductors in pump – probe spectroscopy

Yu.V. Bobyrev, V.M. Petnikova, K.V. Rudenko, V.V. Shuvalov

***Abstract*. It is shown that all the spectral – temporal and temperature anomalies of a nonlinear response of high-temperature superconductors (HTSCs) observed in the pump – probe spectroscopy at high excitation levels can be interpreted taking into account contributions of interband electronic transitions to the dielectric constant of an excited HTSC film with a 'frozen' energy gap in the electronic spectrum. A model is constructed which explains all these 'anomalies' by a drastic decrease in the rates of three-particle nonradiative recombination of excess carriers under strong degeneracy conditions. It is found that this situation takes place due to the specific distribution of the density of electronic states in a HTSC almost immediately after the 'opening' of the energy gap in the electronic spectrum.**

Keywords: *pump – probe spectroscopy, high-temperature superconductors, metastable energy gap, degenerate electronic states, 'anomalous' kinetics of a nonlinear response.*

1. Introduction

In connection with new possibilities that have appeared due to the development of techniques for generating ultrashort laser pulses, the study of ultrafast relaxation of optical excitations in metals [1 – 11], low- [12 – 17] an high-temperature [18 – 34] superconductors (LTSCs and HTSCs) attracts increasing attention. Not least interest in such studies is related to the prospects of the development of ultrafast and supersensitive HTSC bolometers.

Almost all modern experiments in this field are based on the classical version of the pump – probe method for studying the kinetics of variations in the reflection coefficient ΔR [and (or) transmission] of a sample with increasing the delay time τ of a short probe pulse with respect to the instant of 'impact' excitation of the sample by a short pump pulse [18, 20 – 22]. Experimental data are usually interpreted by means of the standard expression [34]

$$\Delta R(\tau) \propto A(T)\left\{H(\tau)\left[1-\exp\left(-\frac{\tau}{\tau_{\rm th}}\right)\right]\exp\left(-\frac{\tau}{\tau_{\rm t}}\right)\right\}, \quad (1)$$

where $A(T)$ is the temperature-dependent nonstationary response amplitude; $H(\tau)$ is the Heaviside function; $\tau_{\rm th}$ and $\tau_{\rm r}$ are the thermalisation and relaxation times of photo-excited carriers (see below). Other methods of nonlinear spectroscopy such as stationary and transient modifications of biharmonic pumping [9, 25, 26], degenerate four-photon spectroscopy [10, 11], terahertz spectroscopy [27 – 29] or hybrid methods with optical excitation and detection of the electric response [16, 17, 23, 24] are used rarely. In this case, other properties (most often spectral) of the nonlinear response are mainly studied [35 – 37].

It was assumed until recently that the basic properties of processes proceeding under such conditions are well known. At the first stage, excited carriers are very rapidly ($\tau_{\rm th} < 10$ fs for the hot electron energy $E_{\rm e} \sim 1$ eV [38, 39]) thermalised by electron – electron (e – e) scattering. In this case, the energy distribution function of thermalised carriers very rapidly returns to the standard Fermi – Dirac distribution with the electron temperature $T_{\rm e}$, which differs both from the initial temperature T_0 of a sample and the temperature $T_{\rm p}$ of its phonon subsystem (lattice) [40]. However, it was found that $\tau_{\rm th} \sim 0.5$ ps even in 'simple' metals (Cu, Ag, Au, etc.) [5, 6, 40], which is caused by restrictions imposed by the Fermi – Dirac statistics on the phase space of the electronic states in the e – e scattering events. Moreover, the theoretically predicted dependence $\tau_{\rm th} \propto T^{-2}$ was not confirmed experimentally, which was explained by the insufficiently low temperature of the sample in experiments [1 – 7, 41].

At the second stage, thermalised carriers are cooled ($T_{\rm e}$ changes) due to electron – phonon (e – p) scattering proceeding for the time $\tau_{\rm r}$. This process was initially described within the framework of the so-called two-temperature model [42], which predicts for 'simple' metals the dependences $\tau_{\rm r} \propto T$ for $T \geqslant T_{\rm D}/5$ and $\tau_{\rm r} \propto T^{-3}$ for $T \ll T_{\rm D}/5$, where $T_{\rm D}$ is the Debye temperature [7, 41, 43 – 45]. However, no substantial increase in $\tau_{\rm r}$ was observed experimentally in the region $T \ll T_{\rm D}/5$, which again was explained by restrictions imposed on the phase space of the electronic states in scattering at low temperatures [1 – 7]. This interpretation was confirmed at the first glance by experiments with LTSC and HTSC films [13 – 15, 19, 30], in which the values of $\tau_{\rm th}$ and $\tau_{\rm r}$ drastically increased in the vicinity of the phase transition to the superconducting state ($T_0 \simeq T_{\rm c}$). It is such behaviour of $\tau_{\rm th}$ and $\tau_{\rm r}$ that was predicted by the theory

Yu.V. Bobyrev, V.M. Petnikova, K.V. Rudenko, V.V. Shuvalov
International Laser Center, M.V. Lomonosov Moscow State University, Vorob'evy gory, 119992 Moscow, Russia;
e-mail: vsh@vsh.phys.msu.su

Received 22 April 2005
Kvantovaya Elektronika **35** (8) 720 – 728 (2005)
Translated by M.N. Sapozhnikov

[12, 46–48], because, simultaneously with the formation of the energy (superconducting) gap in the electronic spectrum, the restrictions imposed on the phase space of the electronic states in scattering events become more rigid.

Experiments have shown that the value of τ_r in LTSCs changes approximately by a factor of five when T_0 changes from 0.980 to $0.995T_c$ [15, 49–51]. In principle, this result agrees with the theoretical prediction [15, 51], according to which $\tau_r \propto \exp[\Delta/(k_B T_c)]$ at low temperatures and a low excitation level, where Δ is the energy gap in the electronic spectrum and k_B is the Boltzmann constant. The value of τ_r in a HTSC changes somewhat weaker (by two–three times) after passing through the point $T_0 \simeq T_c$ [52]. It was found that at a large distance from its peak ($T_0 \simeq T_c$), the relaxation time again increases with decreasing T_0 [31, 33] as $\tau_r \propto T^{-3}$ [33, 53]. This fact was not conclusively explained so far. A similar result was obtained in experiments with heavy fermion metals $YbXCu_4$ (where X = Ag, Cd, In), in which, unlike experiments with nonmagnetic compounds $LuXCu_4$, the value of τ_r increased by more than two orders of magnitude for T_0 lower than the Kondo temperature [41].

All the more paper [34] became unexpected where after a drastic decrease in the pump pulse energy, a principally different result was obtained for a number of cuprates ($La_{2-x}CuO_4$, $Bi_2Sr_2CuO_{6+z}$ doped with lanthanum and $Bi_2Sr_2CaCu_2O_{8+z}$). It was shown that $\tau_r \propto T_0^{-3\pm0.5}$ for all these cuprates at low excitation levels and sufficiently low temperatures, and the value of τ_r begins to increase already in the normal metal phase (for $T_0 > T_c$). In this case, all the above-described features of the behaviour of τ_r in HTSCs in the vicinity of the phase transition point $T_0 \simeq T_c$ do take place, but only at sufficiently high excitation levels. Moreover, these features become more pronounced with increasing the pump pulse energy. The authors [34] assert that, according to the data presented in [31–33, 53–55], the behaviour of τ_r in samples of $YBa_2Cu_3O_{7-\delta}$, $Bi_2Sr_2CuO_{6+\delta}$, $Bi_2Sr_2CaCu_2O_{8+\delta}$, $La_{2-x}Sr_xCuO_4$, $Tl_2Ba_2CuO_{6+\delta}$, and $HgBa_2Ca_2Cu_3O_{8+\delta}$ is similar. No noticeable variations in τ_r in the temperature range from 10 to 280 K was observed in control experiments with metal (Au) films.

The aim of this paper is to explain consistently all the experimental data listed above. Our explanation is based on the four basic assumptions: (i) the energy gap in the electronic spectrum of cuprates is 'frozen' (i.e., it cannot be rapidly destroyed even when the electron temperature T_e substantially differs from the lattice temperature T_p) and a sample is excited to a metastable state [56]; (ii) at high pump levels, the electronic states of HTSC samples are degenerate, i.e., the positions $E_{e,h}^F$ of the Fermi levels for free electrons (quasi-particle states above the energy gap in the electronic spectrum) and holes (similar states, but below the energy gap) do not coincide, the energy between E_e^F and E_h^F drastically increasing with the pump level; (iii) recombination processes of free electrons and holes are nonradiative and three-particle, which drastically decreases the rate of the corresponding processes in the degenerate regime due to the specific energy distribution of the density of electronic states in the HTSC; (iv) the nonlinear response of the HTSC in the pump–probe spectroscopy is caused by interband electronic transitions.

The results of the paper are presented in the following way. In section 2, a simplified closed system of kinetic equations is considered which describes the evolution of thermodynamic parameters $E_{e,h}^F$, $T_{e,h}$, and T_p of the electron, hole, and phonon subsystems of a HTSC film during and after its excitation by a short pump pulse. It is at this stage that we use the first three of the above four assumptions. Then, we present in Section 3 the results of the numerical solution of the system of kinetic equations from Section 2. It is shown that at high excitation levels (in the degeneracy regime), the temporal evolution of the thermodynamic parameters $E_{e,h}^F$, $T_{e,h}$, and T_p strongly changes with the 'opening' of the energy gap in the electronic spectrum caused by a change in the initial temperature T_0 of the film due to a drastic decrease in the recombination rate of free carriers. In Section 4, we describe the model of the electronic part of the nonlinear response of a HTSC, which takes into account contributions from interband electronic transitions to the real (see below) electronic spectrum. Then, we present in Section 5 the results of numerical simulation of the kinetics of the electronic part of the HTSC film nonlinear response obtained by using two modifications of the pump–probe spectroscopy. At this stage, we used the temporal evolution of the thermodynamic parameters $E_{e,h}^F$, $T_{e,h}$, and T_p calculated in Section 3. The most important result of Section 5 is the unusual ('anomalous') dependence of the relaxation time of the nonlinear response of the HTSC film on its initial temperature at high excitation levels. Finally, the results of the paper are summarised in Section 6.

2. System of kinetic equations

The spectrum of one-electron states of a HTSC film with the 'frozen' energy gap is almost completely similar to the electronic spectrum of an intrinsic narrow-gap semiconductor. Therefore, it is convenient to introduce into the problem the two bands separated by the energy gap Δ (an analogue of the valence and conduction bands in a narrow-gap semiconductor) and consider the evolution of concentrations $N_{e,h}$ of free electrons and holes, respectively, in these bands. If we now assume that the rate of intraband thermalisation of free carriers (intraband electron–electron relaxation) is infinitely high, then the energy distributions of electrons and holes in these bands can be considered quasi-equilibrium at any instant t. In this case, the description of the evolution of the system becomes parametrical and is reduced to the introduction of the time dependences of the instantaneous values of $E_{e,h}^F$ and $T_{e,h}$ characterising the position of the Fermi level and temperature in subsystems of free electrons and holes. It is these instantaneous values of $E_{e,h}^F$ and $T_{e,h}$ that should be substituted to the standard Fermi–Dirac distribution function $f_F(E_{e,h}; E_{e,h}^F, T_{e,h})$ at each instant t. The concentrations $N_{e,h}$ of free electrons and holes and the energy densities $Q_{e,h}$ stored in the two corresponding subsystems (their 'heat' storage) are determined by the conventional expressions

$$N_{e,h} = N_c \int_0^\infty f_F(E_{e,h}; E_{e,h}^F, T_{e,h}) g_{e,h}(E_{e,h}; \Delta) dE_{e,h}, \quad (2)$$

$$Q_{e,h} = N_e \langle E_{e,h} \rangle = N_c \int_0^\infty E_{e,h} f_F(E_{e,h}; E_{e,h}^F, T_{e,h}) g_{e,h}(E_{e,h}; \Delta) dE_{e,h}, \quad (3)$$

where N_c is the cell density; the functions $g_{e,h}(E_{e,h}; \Delta)$ describe the density of electronic states in the corresponding bands for a fixed energy gap Δ in the electronic spectrum; and $\langle E_{e,h} \rangle$ is the average energy of a free electron and a hole. Taking into account the symmetry of the problem and that all the processes of interest to us are pair (photogeneration of free electrons and holes and their recombination), we will always assume below that the states of the electron and hole subsystems are identical at each instant t and

$$g(E; \Delta) \equiv g_e(E; \Delta) = g_h(E; \Delta),$$
$$E^F \equiv E_e^F = E_h^F,\ T_e = T_h,\ \langle E_e \rangle = \langle E_h \rangle,\ N_e = N_h,\ Q_e = Q_h. \tag{4}$$

Then, to describe the evolution of the electron and hole subsystems of the HTSC film, it is sufficient to have the kinetic equations for the concentration N_e and to know the energy storage Q_e in the subsystem of free electrons.

The kinetic equation for N_e can be written assuming that the photogeneration and recombination of free carriers is strictly pair:

$$\frac{dN_e}{dt} = [1 - f_F(\langle E_e \rangle; E^F, T_e)] P_p(t) \frac{N_e}{Q_e} \frac{\hbar\omega}{2} - \gamma_{eh}^R (N_e^2 - N_s^2). \tag{5}$$

Here, $P_p(t)$ is the instantaneous flux density of absorbed photons of the pump pulse with the energy $\hbar\omega$; $\gamma_{eh}^R = \gamma_{ehp}^R + \gamma_{ehe}^R$ is the constant of nonradiative pair recombination of free electrons and holes, which is determined by the sum of constants γ_{ehp}^R and γ_{ehe}^R describing three-particle processes involving a phonon and another electron (hole), respectively, and can depend on Δ, E^F, temperatures T_e and T_p of the electron and phonon subsystems, N_e, and other parameters (see below) [57];

$$N_s = N_c \int_0^\infty f_F(E_e; E_0^F, T_p) g(E_e; \Delta) dE_e$$

is a quasi-equilibrium concentration of free electrons and holes for $E^F = E_0^F$ and $T_e = T_p \neq T_0$. The first term in Eqn (5) describes the photogeneration of free carriers taking into account that absorption of each pump photon generates hot electrons in the conduction band, which undergo the instantaneous interband e–e scattering resulting, in the absence of competition with other process, in the creation $\hbar\omega/(2\langle E_e \rangle)$ of already thermalised free electrons and holes (with the average energy $\langle E_e \rangle = Q_e/N_e$). The factor $[1 - f_F(\langle E_e \rangle; E^F, T_e)]$ in this term, which takes into account the competition between interband and intraband e–e scattering, changes from 1/2 (for $E^F \ll \Delta/2$) to 1 (in the absence of degeneracy).

A third quasi-particle involved in the pair recombination of a free electron and a hole cannot be arbitrary because the initial (E') and final ($E'' \simeq E' + 2\langle E_e \rangle$, as follows from the energy conservation law) energy states of this particle cannot be completely empty and completely occupied, respectively. In the case of degeneracy (when the nonequilibrium position of the Fermi level $E^F \geqslant \Delta/2$ and the level lies in the conduction band), the concentration of quasi-particles that can be involved in recombination drastically decreases due to a sharp peak in the distribution of the density of states $g(E_e)$ in the HTSC in the vicinity of the point $E_e = \Delta/2$. The larger the gap width Δ, the higher the degeneracy degree and the lower the electron temperature T_e, the stronger this effect should be manifested. Below, this effect was taken into account with the help of the expression

$$\gamma_{ehe}^R \simeq \tilde{\gamma}_{ehe}^R \tilde{N}_e, \tag{6}$$

where $\tilde{\gamma}_{ehe}^R$ is a constant independent of the concentration of third quasi-particles and

$$\tilde{N}_e \simeq N_c \int_0^\infty dE' f_F(E'; E^F, T_e)[1 - f_F(E' + 2\langle E_e \rangle; E^F, T_e)]$$
$$\times g(E') g(E' + 2\langle E_e \rangle) \leqslant N_e. \tag{7}$$

If the third quasi-particle involved in recombination is an acoustic photon, the rate of the corresponding process described by the constant γ_{ehp}^R should also sharply decrease with increasing the total energy $2\langle E_e \rangle$ of recombining particles because acoustic phonons with the maximum admissible energy E_{max} cannot take away the energy of these particles. For the standard dispersion dependence model [57]

$$E_{ph} \simeq E_{max} \sin\left(\frac{\pi}{2} \frac{K}{K_{Br}}\right) \tag{8}$$

in the isotropic approximation, this results in the appearance of the additional correction factor in the expression for the recombination constant

$$\gamma_{ehp}^R \to \gamma_{ehp}^R(\langle E_e \rangle)$$
$$= \tilde{\gamma}_{ehp}^R \int_0^{E_{max}} dE_{ph} F(E_{ph}; T_p) G(E_{ph}) G(E_{ph} + 2\langle E_e \rangle), \tag{9}$$

where $\tilde{\gamma}_{ehp}^R$ is a constant independent of the lattice temperature T_p and energy $\langle E_e \rangle$ of recombining free carriers; E_{ph} and K are the energy and momentum of an acoustic phonon; E_{max} is the maximum energy of the latter for $K = K_{Br}$ (at the edge of the Brillouin zone);

$$F(E_{ph}; T_p) = \left[\exp\left(\frac{E_{ph}}{k_B T_p}\right) - 1\right]^{-1}, \tag{10}$$

$$G(E_{ph}) = \begin{cases} (E_{max}^2 - E_{ph}^2)^{-1} \arcsin\left(\dfrac{E_{ph}}{E_{max}}\right) & \text{for } E_{ph} \leqslant E_{max}, \\ 0 \quad \text{for } E_{ph} > E_{max} \end{cases} \tag{11}$$

is the distribution function and density of phonon states, respectively.

We will describe the evolution of the energy density ('heat' storage) Q_e in the electron subsystem by another kinetic equation, which can be easily written by representing Q as a function of two variables N_e and $\langle E_e \rangle$:

$$Q_e = Q_e(N_e, \langle E_e \rangle) = N_e \langle E_e \rangle$$
$$= N_e \int_0^\infty E_e f_F(E_e; E^F, T_e) g(E_e; \Delta) dE_e. \tag{12}$$

By varying expression (12) over N_e and $\langle E_e\rangle$ (i.e., assuming in fact that these two variables are independent), we obtain at once the equation

$$\frac{dQ_e}{dt} = \frac{d}{dt}(N_e\langle E_e\rangle) = \frac{dN_e}{dt}\bigg|_{\langle E_e\rangle=\text{const}}\langle E_e\rangle + N_e\frac{d\langle E_e\rangle}{dt}\bigg|_{N_e=\text{const}}$$

$$= \frac{Q_e}{N_e}\frac{dN_e}{dt} - N_e\gamma_{ep}^{(Q)}\left[\langle E_e(E^F,T_e)\rangle - \langle E_e(E^F,T_p)\rangle\right]$$

$$= P_p(t)\frac{\hbar\omega}{2} - \frac{Q_e}{N_e}\gamma_{ehp}^{R}\left(N_e^2 - N_s^2\right) - \gamma_{ep}^{(Q)}\left(Q_e - \frac{N_e}{N_{es}}Q_{es}\right). \quad (13)$$

Here, we used in transformations the so-called relaxation approximation

$$\frac{d\langle E_e\rangle}{dt}\bigg|_{N_e=\text{const}} = -\gamma_{ep}^{(Q)}\left[\langle E_e(E^F,T_e)\rangle - \langle E_e(E^F,T_p)\rangle\right]$$

$$\simeq -\gamma_{ep}^{(Q)}\left(\frac{Q_e}{N_e} - \frac{Q_{es}}{N_{es}}\right), \quad (14)$$

where the constant $\gamma_{ep}^{(Q)}$ describes the relaxation rate of the average energy of a free electron (in fact, T_e) within the framework of the two-temperature Allen model [38] and depends on $T_{e,p}$ because the specific heats $c_{e,p}$ of the electron and phonon subsystems depend on $T_{e,p}$;

$$Q_{es} = N_{es}\int_0^\infty E_e f_F(E_e;E^F,T_p)g(E_e;\Delta)dE_e,$$

$$N_{es} = N_c\int_0^\infty f_F(E_e;E^F,T_p)g(E_e;\Delta)dE_e$$

are the energy density and concentration of free electrons, respectively, at the equilibrium temperature $T_e = T_p$ for nonequilibrium position of the Fermi level ($E^F \neq E_0^F$). The first term of kinetic equation (13) for Q_e takes into account the energy 'income' to the electron subsystem due to absorption of pump photons, the second term describes the energy 'escape' from the electron subsystem due to recombination of free electrons and holes involving phonons, and the third term describes the cooling of the electron subsystem due to transfer of the kinetic energy of free carriers to the phonon subsystem. In fact, the form of Eqn (13) proves that the probability of recombination processes is the same for all quasi-particles and is independent of their energy. It is in this case that each recombination event of a free electron and a hole should be accompanied by the taking away of the same portion of energy $\langle E_e\rangle = Q_e/N_e$ from the total energy of the electron system in the conduction band.

The energy exchange with a thermostat, whose role is played by a substrate at temperature T_s, can be descried by another kinetic equation for the energy density ('heat' storage) Q_p in the phonon subsystem. Taking into account the balance between the energy income and escape and the principle of detailed balancing, this equation in the relaxation approximation also has a simple form

$$\frac{dQ_p}{dt} = 2\frac{Q_e}{N_e}\gamma_{ehp}^{R}(N_e^2 - N_s^2) + 2\gamma_{ep}^{(Q)}(Q_e - Q_{es})$$

$$-\gamma_{ps}^{(Q)}(Q_p - Q_{ps}). \quad (15)$$

Here, $Q_{p,ps} = c_p T_{p,ps}$, where T_p and $T_{ps} = T_s$ are the current and equilibrium temperatures of the phonon subsystem. We can assume in calculations that due to a very large heat capacity of the thermostat (substrate) its temperature does not change and $T_s \equiv T_0$. Note that the relaxation rate $\gamma_{ps}^{(Q)}$ of the heat excess in Eqn (15) can also depend in principle on T_p and T_s because the specific heat c_p of the phonon subsystem depends on temperature.

3. Solution of the system of kinetic equations

We assumed in all numerical calculations that the initial values $E^F(t=0) = E_0^F = 0$ and $T_e(t=0) = T_0$ determine the initial conditions for the system of kinetic equations

$$N_e(t=0) = N_c\int_0^\infty f_F(E_e;E^F=0,T_e=T_0)g(E_e;\Delta)dE_e, \quad (16)$$

$$Q_e(t=0) = N_e\int_0^\infty E_e f_F(E_e;E^F=0,T_e=T_0)g(E_e;\Delta)dE_e, \quad (17)$$

$$Q_p(t=0) = c_p T_0. \quad (18)$$

The energy gap in the electronic spectrum of the HTSC film was assumed a constant dependent only on the initial temperature T_0 and the superconducting transition critical temperature T_c ('frozen' gap):

$$\Delta = \Delta(T_0) \equiv \begin{cases} 3.12k_B T_c(1 - T_0/T_c)^{1/2} \text{ for } T_0 \leqslant T_c, \\ 0 \text{ for } T_0 > T_c. \end{cases} \quad (19)$$

Expression (19) corresponds to the so-called weak coupling limit in the BCS theory. The current values $E^F(t)$ and $T_e(t)$ were determined by solving the system of two integral equations

$$N_e(t\neq 0) = N_c\int_0^\infty f_F(E_e;E^F,T_e)g(E_e;\Delta)dE_e, \quad (20)$$

$$Q_e(t\neq 0) = N_e\int_0^\infty E_e f_F(E_e;E^F,T_e)g(E_e;\Delta)dE_e. \quad (21)$$

For initial temperatures $T_0 > T_c$, the distribution of the density of electronic states $g(E_e;\Delta\equiv 0)$ was calculated from the standard expression [58]

$$g(E_e;\Delta\equiv 0) = \frac{1}{4\pi^3}\oiint_{E_e=\text{const}}\frac{dS}{|\nabla_{\boldsymbol{k}}E_e(\boldsymbol{k})|} \quad (22)$$

using the values of $E_e(\boldsymbol{k})$ for the real (calculated by the pseudopotential method) band structure of La_2CuO_4 [59] (Fig. 1a). Here, $E_e(\boldsymbol{k})$ describes the shape of the conduction band of La_2CuO_4, i.e., the dependence of the electron energy E_e on the quasi-momentum $\boldsymbol{k}$; integral (22) is taken over the surface S with the energy $E_e = \text{const}$. Upon integration, data [59] (taking the symmetry into account) were interpolated to the entire first Brillouin zone by the method described in [60]. As expected, the dependence $g(E_e;\Delta\equiv 0)$ calculated in this way had a distinct narrow peak in the vicinity of the point $E_e = 0$. Then, this dependence was approximated by a smooth analytic function with an accuracy of 99.5 % in the energy range $|E_e - E_0^F| \leqslant 1$ eV. For initial temperatures $T_0 \leqslant T_c$, we

'introduced' into distribution (22) the energy gap with the so-called s symmetry, i.e., electronic states with the energy lying within a layer of width $2\Delta(T_0)$ in the vicinity of E_0^{F} were redistributed over the Brillouin zone in accordance with the expression

$$g(E_{\mathrm{e}};\Delta) = 0 \quad \text{for} \quad E_{\mathrm{e}} < \Delta,$$

$$g(E_{\mathrm{e}};\Delta) = g(E_{\mathrm{e}};\Delta \equiv 0) + \frac{1}{k_{\mathrm{B}}T_0}\exp\left(-\frac{E_{\mathrm{e}}}{k_{\mathrm{B}}T_0}\right) \times \int_0^{\Delta(T_0)} g(E_{\mathrm{e}};\Delta \equiv 0)\mathrm{d}E_{\mathrm{e}} \quad \text{for} \quad E_{\mathrm{e}} \geqslant \Delta. \tag{23}$$

The evolution of the calculated distribution of the density of electronic states $g(E_{\mathrm{e}})$ depending on T_0 is shown in Fig. 1b, which clearly demonstrates the instant of the appearance of the energy gap at the point $T_0 = T_{\mathrm{c}}$.

The system of differential equations (5), (13), (15) was solved by the fourth-order Runge–Kutta method. The numerical values of control parameters corresponded more or less to some standard conditions for most of real spectroscopic experiments. We assumed that the $\sim$200-nm thick HTSC film absorbs 30 % of the total energy (4×10^{-7} J) of the 30-fs, 800-nm pump pulse of a Ti : sapphire laser. The diameter of the focal spot was assumed to be 150 μm, while the values of other parameters (the phase transition temperature $T_{\mathrm{c}} = 90$ K, the specific heat of the film $c_{\mathrm{p}} = 0.9$ J cm^{-3} K^{-1}, the rate of relaxation of the heat excess to the substrate $\gamma_{\mathrm{ps}}^{(Q)} = 5 \times 10^{-3}$ ps^{-1}, $E_{\max} \simeq 15$ meV) were approximately the same as those for an $YBa_2Cu_3O_{7-\delta}$ HTSC film on a $SrTiO_3$ substrate. The two remaining (fitting) parameters $\tilde{\gamma}_{\mathrm{ehe}}^{\mathrm{R}}$ and $\tilde{\gamma}_{\mathrm{ehp}}^{\mathrm{R}}$ were varied to obtain the relaxation time τ_{r} of the nonlinear response equal to $\sim$0.3 and 1.5 ps at the initial temperatures $T_0 = 100$ and 40 K, respectively, which approximately corresponds to the data of real experiments.

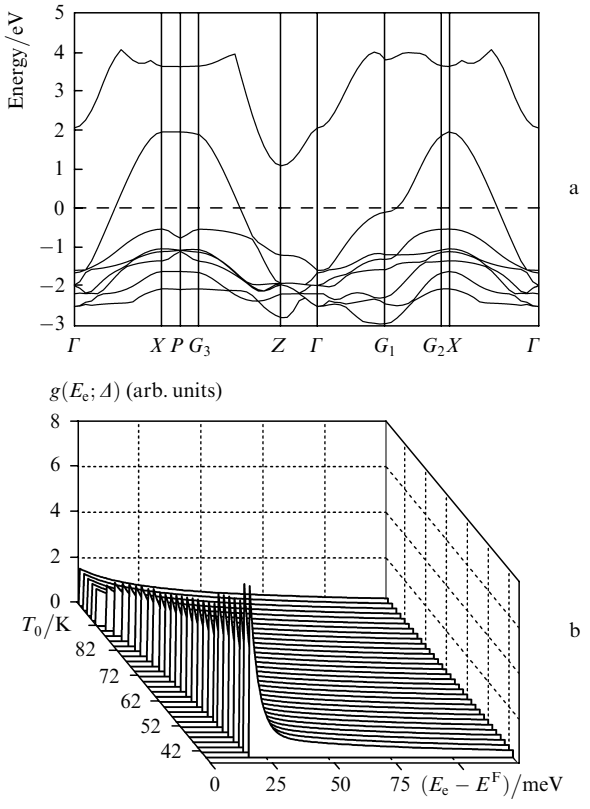

Figure 1. Band structure of La_2CuO_4 at room temperature according to [59] (a) and the distributions of the density of electronic states $g(E_{\mathrm{e}};\Delta)$ in the spectrum of the HTSC sample at different initial temperatures T_0 (b). The formation temperature of the energy gap in the electronic spectrum corresponds to the phase transition point $T_0 = T_{\mathrm{c}}$. The letters Γ, G_{1-3}, P, X, and Z denote the standard symmetry points of the Brillouin zone.

Figure 2 shows a drastic transformation of the kinetics of the instant shift of the Fermi level $\Delta E^{\mathrm{F}}(t) = E_{\mathrm{e}}^{\mathrm{F}}(t) - E_0^{\mathrm{F}}$ and of instant variations in the electron temperature $\Delta T_{\mathrm{e}}(t) = T_{\mathrm{e}}(t) - T_0$, the concentration $\Delta N_{\mathrm{e}}(t) = N_{\mathrm{e}}(t) - N_0$ of free carriers in the conduction band separated by the energy gap, and the lattice temperature $\Delta T_{\mathrm{p}}(t) = T_{\mathrm{p}}(t) - T_0$ of the HTSC film depending on its initial temperature T_0, calculated by using the above expressions. It is easy to verify that absorption of the 30-fs, 4×10^{-7}-J pump pulse by the HTSC film causes drastic changes in the kinetics of the instant values of almost all thermodynamic parameters of the film upon variation of the initial temperature T_0 in the vicinity of the 'opening' temperature of the energy gap in the electronic spectrum. It is obvious that this simply will not fail to affect the following temporal evolution of the nonlinear response. In this case, the type of temporal variations in the instant constants of pair recombination involving electrons [$\gamma_{\mathrm{ehe}}^{\mathrm{R}}(t)$, Fig. 3a] and acoustic phonons [$\gamma_{\mathrm{ehp}}^{\mathrm{R}}(t)$ Fig. 3b] at different initial temperatures T_0 of the film conclusively implies the principal role of these processes.

4. Model of the electron part of a nonlinear response

We will assume below that the nonlinear response of a HTSC film in the pump–probe method is determined by the change $\delta\varepsilon$ in the initial complex dielectric constant $\varepsilon_0 = \varepsilon(T_0)$ of the film, which is caused by the deviation of the thermodynamic parameters $E_{\mathrm{e}}^{\mathrm{F}}$ and T_{e} of the electron subsystem from their equilibrium values produced by a pump pulse. Because the reflection coefficient R at the air–HTSC film interface is determined by the dielectric constant ε of the film according to the expression

$$R = \left(\frac{\sqrt{\varepsilon} - 1}{\sqrt{\varepsilon} + 1}\right)^2, \tag{24}$$

by substituting $R = R_0 + \delta R$ and $\varepsilon = \varepsilon_0 + \delta\varepsilon$ into (24) and using the first correction in $\delta\varepsilon$ to the initial reflection coefficient R_0, we obtain

$$\delta R = 2R_0 \frac{\delta\varepsilon}{\sqrt{\varepsilon_0}(\varepsilon_0 - 1)}. \tag{25}$$

This approach is almost always used to interpret the results of any real experiment. However, below, unlike papers [18, 19, 21, 27, 30–34, 47, 52, 53], where only absorption by free carriers (excited by the pump pulse) was considered at the probe stage, we will calculate $\delta\varepsilon$ taking into account the electron part of the instant linear response ε of the HTSC film caused only by interband electronic transitions. In principle, the authors of papers [20, 22, 48] attempted to realise the same procedure within the framework of rather

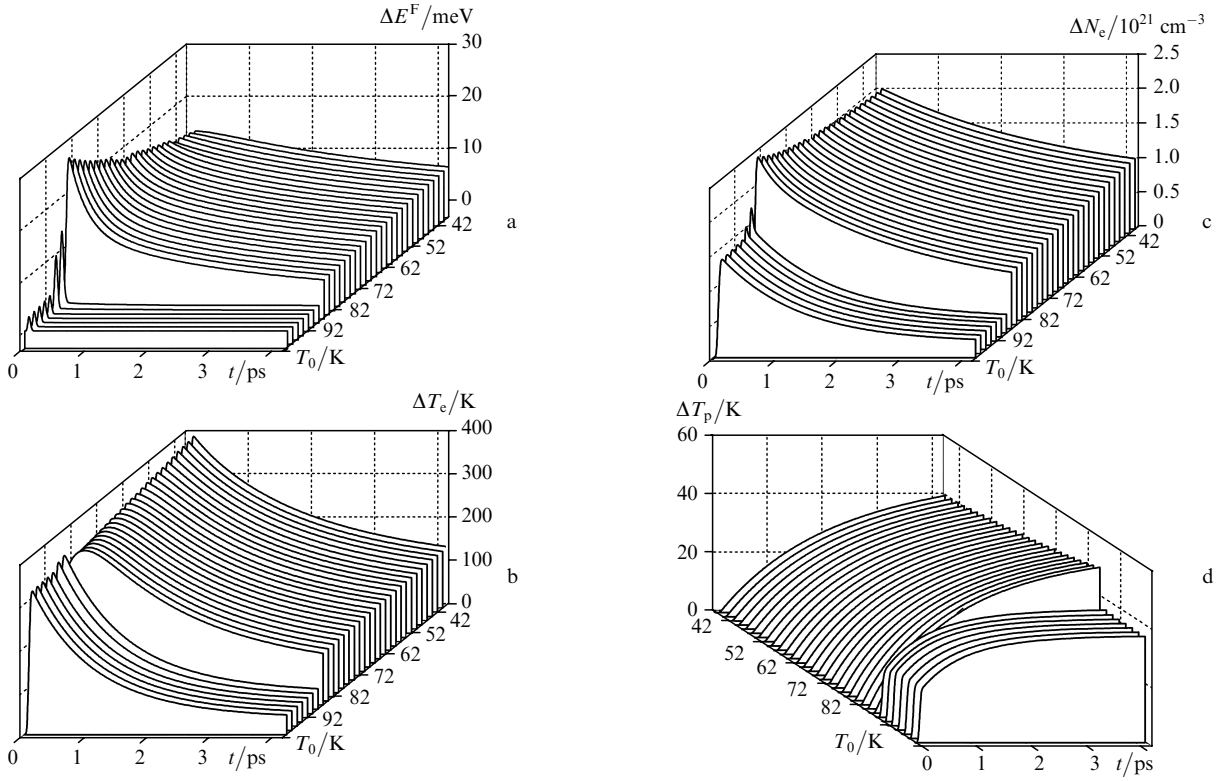

Figure 2. Transformation of the kinetics of instant variations in the Fermi level position $\Delta E^{\mathrm{F}}(t)$ (a), the temperature $\Delta T_{\mathrm{e}}(t)$ of the electron subsystem (b), the total initial electron concentration $\Delta N_{\mathrm{e}}(t)$ in the conduction band (c), and the lattice temperature ΔT_{p} (d) caused by the pump pulse upon changing the initial temperature T_0 of the HTSC sample.

rough qualitative models; however, it will be clear below that the model constructed in this section is substantially more exact and realistic.

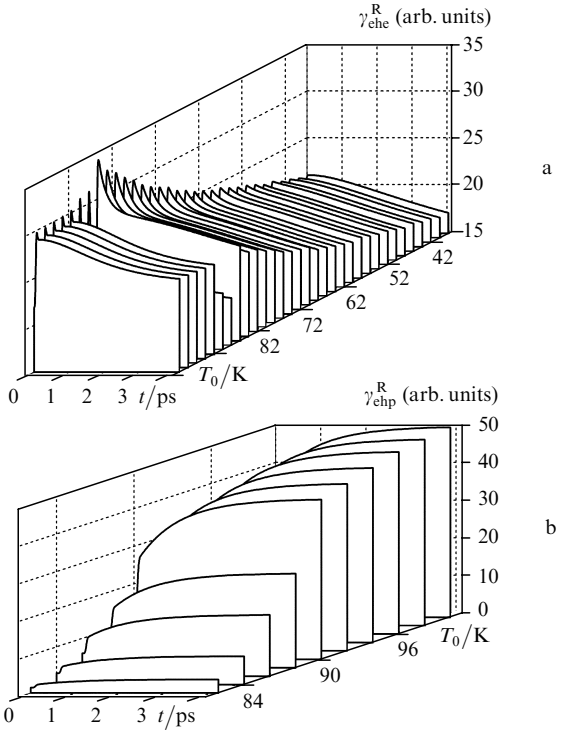

Figure 3. Changes in the kinetics of the rates of three-particle recombination $\gamma^{\mathrm{R}}_{\mathrm{ehe}}(t)$ (a) and $\gamma^{\mathrm{R}}_{\mathrm{ehp}}$ (b) caused by absorption of the pump pulse upon changing the initial temperature T_0.

We will neglect below the dependences of R_0 and ε_0 in (25) on the probe-pulse wavelength in a comparatively narrow spectral interval 620–680 nm of interest to us and calculate the quantity $\delta\varepsilon$ by using the standard expression

$$\varepsilon \sim \sum_{i \neq i'} \iint \frac{|d_{i,i'}(\boldsymbol{k},\boldsymbol{k}')|^2 n_i(\boldsymbol{k})[1-n_{i'}(\boldsymbol{k}')]}{\omega - \Omega_{i,i'}(\boldsymbol{k},\boldsymbol{k}') + \mathrm{i}\Gamma_{i,i'}(\boldsymbol{k},\boldsymbol{k}')}\,\mathrm{d}\boldsymbol{k}\mathrm{d}\boldsymbol{k}'. \qquad (26)$$

Here, $\boldsymbol{k}$ is the electron quasi-momentum; the subscripts i and i' numerate the electronic bands involved in the $(i,\boldsymbol{k}) \to (i',\boldsymbol{k}')$ transition with the dipole moments $d_{i,i'}(\boldsymbol{k},\boldsymbol{k}')$; $n_i(\boldsymbol{k})$ is the occupation number of the $(i,\boldsymbol{k})$ state, which is determined by the Fermi–Dirac distribution; $\Omega_{i,i'}(\boldsymbol{k},\boldsymbol{k}')$ is the resonance transition frequency; and $\Gamma_{i,i'}(\boldsymbol{k},\boldsymbol{k}')$ is the relaxation rate of interband polarisation. Integration over $\boldsymbol{k}$ и $\boldsymbol{k}'$ in (26) is performed within the first Brillouin zone, and summation over subscripts i and i' involves all the allowed electronic bands. Taking into account that the photon momentum is small, we will assume that all the $(i,\boldsymbol{k}) \to (i',\boldsymbol{k}')$ electronic transitions are direct ($\boldsymbol{k} = \boldsymbol{k}'$) and pass in (26) to single integration over $\boldsymbol{k}$ by using the notation $d_{i,i'}(\boldsymbol{k},\boldsymbol{k}') = d_{i,i'}(\boldsymbol{k})$, $\Gamma_{i,i'}(\boldsymbol{k},\boldsymbol{k}') = \Gamma_{i,i'}(\boldsymbol{k})$ and $\Omega_{i,i'}(\boldsymbol{k},\boldsymbol{k}') = \Omega_{i,i'}(\boldsymbol{k})$. The resonance transition frequencies are described by the standard expressions $\Omega_{i,i'}(\boldsymbol{k}) = E_{i'}(\boldsymbol{k}) - E_i(\boldsymbol{k})$, where $E_i(\boldsymbol{k})$ is the electron energy in the $(i,\boldsymbol{k})$ state normalised to Planck's constant.

We used the following simplifications in numerical calculations. As in [11, 60], we assumed that $d_{i,i'}(\boldsymbol{k}) = d$ and $\Gamma_{i,i'}(\boldsymbol{k}) = \Gamma = 5 \times 10^{12}$ s^{-1} are constants independent of i, i', and $\boldsymbol{k}$. The resonance frequencies $\Omega_{i,i'}(\boldsymbol{k})$ of electronic transitions in (26) were calculated by interpolating the known data about the band structure of La_2CuO_4 at

room temperature [59] to the first Brillouin zone taking into account the symmetry and periodicity. The subsequent cooling of a sample down to temperature $T_0 \leqslant T_c$ was simulated by the forced introduction of the 'frozen' energy gap (19) to the spectrum of one-electron states obtained in this way, i.e., by the replacement $E_e(\boldsymbol{k}) \to E_0^F \pm \{[E_e(\boldsymbol{k}) - E_0^F]^2 + \Delta(T_0)^2\}^{1/2}$ for $E_e(\boldsymbol{k}) > E_0^F$ and $E_e(\boldsymbol{k}) < E_0^F$, respectively [61]. By using this procedure, we performed the redistribution of the density of electronic states in the model band structure of the HTSC film in the vicinity of the Fermi level, which simulated the phase transition. Both the above-described procedures allowed us to include the real (i.e., known from the literature) electronic spectrum of the HTSC film to our model, which resulted in a drastic decrease in the number of free (fitting) parameters of the model. Integration in (26) was performed by the singularity method [62] over all the state bands [59] lying in the energy range $|E_e \pm E_0^F| \leqslant 2.5$ eV. The instant values of ε were calculated by assuming that the occupation numbers $n_i(\boldsymbol{k})$ of the electronic states in expression (26) are specified by the Fermi–Dirac distribution $f_F(E_e; E_e^F, T_e)$ with the instant values of the thermodynamic parameters $E_e^F(t)$ and $T_e(t)$ calculated by the method described in Section 3.

5. Simulation of a nonlinear response

In this section, we present the results obtained by numerical simulation of the kinetics of the electron part of the nonlinear response of a HTSC film [see (26)] by using two modifications of the pump–probe method at high excitation levels. As in Section 3, we assume that the thermodynamic parameters E_e^F and T_e of the electron subsystem of the HTSC film with the same characteristics (Section 3) vary in time after absorption of 30 % (the film thickness is ~200 nm) of the energy (4×10^{-7} J) of the 30-fs, 800-nm pump pulse focused into a spot of diameter 150 μm. However, we will assume in the first of the situations considered below (Fig. 4) that the instant state of the HTSC film is probed at the pump pulse wavelength (800 nm), i.e., the experimental data similar to those described in papers [18, 19, 21, 27, 30–34, 47, 52, 53] will be simulated. Then (Fig. 5), we will assume that the experimental situation is different and the instant state of the sample is also probed by a short pulse but at different wavelengths (for example, by a broadband supercontinuum) in the range 620–680 nm, which corresponds to the experimental conditions described in papers [20, 22, 48]. This modification of the pump–probe method is often called spectrochronography [63].

Figure 4a illustrates a drastic transformation of the kinetics of the modulus of the dielectric constant $\Delta\varepsilon(t) = |\varepsilon(t)| - |\varepsilon_0|$ of the HTSC film upon variations of its initial temperature in the vicinity of the phase transition point $T_0 \sim T_c$ and probing of the excited film at the pump-pulse wavelength. The exponential approximation of the initial part (the region of small time delays of the probe pulse) of the family of kinetic curves $\Delta\varepsilon(t, T_0)$ presented in the figure gives a nontrivial dependence of the relaxation time $\tau_{\Delta\varepsilon}$ of the electron part of the nonlinear response on T_0 (Fig. 4b) with a distinct abrupt step (a jump of $\tau_{\Delta\varepsilon}$ at $T_0 \simeq 86$ K, i.e., slightly lower than the phase transition temperature $T_c \simeq 90$ K). One can easily see that both the transformation of the dependences $\Delta\varepsilon(t)$ with changing T_0 (Fig. 4a), including the two-exponential relaxation of $\Delta\varepsilon$ at T_0 in

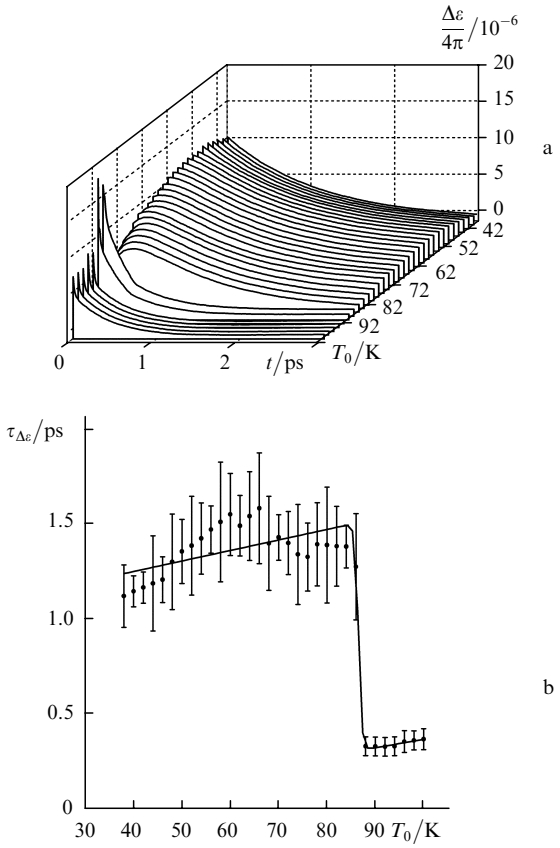

Figure 4. Transformation of the kinetics of variations of the modulus of the dielectric constant $\Delta\varepsilon(t)$ of the HTSC sample caused by the pump pulse upon varying the initial temperatures T_0 (a) and the dependence of the relaxation time $\tau_{\Delta\varepsilon}$ on T_0 upon probing the sample at the pump wavelength (b).

the vicinity of the phase transition point T_c, and the calculated dependence $\tau_{\Delta\varepsilon}(T_0)$ (Fig. 4b) almost exactly reflect all the 'anomalies' of the nonlinear response kinetics observed in real experiments [32, 34, 41, 47, 52, 53]. Compared to the results of real experiments, the only peculiarity of the dependence $\tau_{\Delta\varepsilon}(T_0)$ that we have 'lost' in our simulation is the absence of a narrow peak at the top of the step (Fig. 4b). It seems that this is caused by the approximation we used, according to which all the relaxation rates in (5), (13)–(15) depend only on average energies. Note also that all the above 'anomalies' of the nonlinear response kinetics within the framework of our model completely disappear with decreasing the pump-pulse energy (i.e., when the Fermi levels $E_{e,h}^F$ of free electrons and holes coincide with the real Fermi level E_0^F).

In spectrochronography, i.e., when the instant state of a HTSC film is probed by a supercontinuum pulse, the situation becomes much more complicated. Figure 5 shows the calculated transformation of the spectral dependences of variations in the modulus of the dielectric constant $\Delta\varepsilon(\lambda) = |\varepsilon(\lambda)| - |\varepsilon_0|$ of the HTSC sample, caused by absorption of a pump pulse, in the range 620–680 nm for initial temperatures $T_0 = 100$ and 40 K with increasing the probe-pulse delay. Although our calculations showed that the relaxation time $\tau_{\Delta\varepsilon}$ also undergoes a jump with decreasing the initial temperature of the HTSC film down to the same value $T_0 \simeq 86$ K, as in Fig. 4, and a similar step is formed in the dependences $\tau_{\Delta\varepsilon}(T_0)$ for all λ, the further run of the

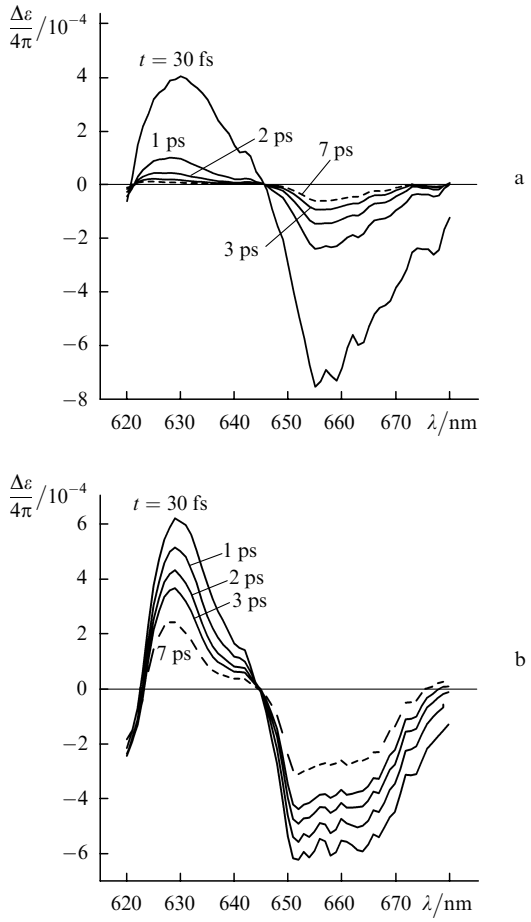

Figure 5. Spectral dependences of variations in the modulus of the dielectric constant $\Delta\varepsilon(\lambda)$ of the HTSC sample caused by absorption of the pump pulse upon probing in the wavelength range 620–680 nm at initial temperatures $T_0 = 100$ (a) and 40 K (b) at different instants.

curves $\tau_{\Delta\varepsilon}(T_0)$ at low temperatures ($T_0 < 86$ K) depends on λ due to a gradual displacement of local extrema $\Delta\varepsilon$ along the wavelength axis with increasing the probe-pulse delay (Fig. 5b). As in real experiments [20, 22, 48], there exist singularities on the wavelength axis λ in the vicinity of which $\Delta\varepsilon \equiv 0$, and it is these singularities that separate spectral regions with the opposite signs of the changes $\Delta\varepsilon$ induced by the pump pulse (Fig. 5b). Note here that this result is not so trivial as it may seem, because we deal with a simultaneous vanishing of both the real and imaginary parts of a nonlinear response. Therefore, in our opinion, the presence of such singularities on the wavelength axis λ can be caused only by a change in the phase relations between the two interfering components of the dielectric constant, which appear due to the frequency degeneracy of probing (see, for example, [61]).

6. Conclusions

We have shown that all the known spectral–temporal and temperature 'anomalies' of the behaviour of the nonlinear response $\Delta\varepsilon$ of HTSC films, which were observed in papers [18–22, 27, 30–34, 47, 48, 52, 53] at high excitation levels by the methods of pump–probe spectroscopy can be interpreted within the framework of a simple and physically clear model with the minimum number of free (fitting) parameters. This model, based on the consideration of the contribution of interband electronic transitions to the dielectric constant ε of the excited HTSC film with the 'frozen' (metastable [56]) energy gap in the real (known from the literature [59]) electronic spectrum, explains all these 'anomalies' by a drastic decrease in the rates of three-particle nonradiative relaxation of excess carriers under the conditions of a strong degeneracy. In this case, the drastic decrease in the rate constants γ_{ehp}^{R} and γ_{ehe}^{R} of pair recombination occurs almost at once after the 'opening' of the energy gap in the electronic spectrum of the HTSC film (after decreasing the initial temperature T_0 of the HTSC film slightly below the phase transition point T_c) due to the quite unusual shape of the distribution function $g(E_e)$ of the density of electronic states (compared to the electronic spectrum of narrow-gap semiconductors).

Acknowledgements. This work was supported by the Program of the President of the Russian Federation (Grant Nos NSh-1583.2003.2 and MK-1328.2004.2).

References

1. Rosei R. et al. *Phys. Rev. B*, **10**, 484 (1974).
2. Eesley G.L. *Phys. Rev. Lett.*, **51**, 2140 (1983).
3. Elsayed-Ali H.E. et al. *Phys. Rev. Lett.*, **58**, 1212 (1987).
4. Schoenlein R.W. et al. *Phys. Rev. Lett.*, **58**, 1680 (1987).
5. Fann W.S. et al. *Phys. Rev. B*, **46**, 13592 (1992).
6. Sun C.K. et al. *Phys. Rev. B*, **48**, 12365 (1993).
7. Groeneveld R.H.M. et al. *Phys. Rev. B*, **51**, 11433 (1995).
8. Dobryakov A.L. et al. *Physica Scripta*, **60**, 572 (1999).
9. Petnikova V.M. et al. *Kvantovaya Elektron.*, **28**, 69 (1999) [*Quantum Electron.*, **29**, 626 (1999)].
10. Kuznetsova L.P. et al. *Kvantovaya Elektron.*, **30**, 175 (2000) [*Quantum Electron.*, **30**, 175 (2000)].
11. Bobyrev Yu.V. et al. *Kvantovaya Elektron.*, **32**, 789 (2002) [*Quantum Electron.*, **32**, 789 (2002)].
12. Rothwarf A., Taylor B.N. *Phys. Rev. Lett.*, **19**, 27 (1967).
13. Owen C.S., Scalapino D.J. *Phys. Rev. Lett.*, **28**, 1559 (1972).
14. Parker W.H., Williams W.D. *Phys. Rev. Lett.*, **29**, 924 (1972).
15. Schuller I., Gray K.E. *Phys. Rev. Lett.*, **36**, 429 (1976).
16. Bluzer N. *J. Appl. Phys.*, **71**, 1336 (1992).
17. Forrester M.G. *Appl. Phys. Lett.*, **53**, 1332 (1988).
18. Brorson S.D. et al. *Phys. Rev. Lett.*, **64**, 2172 (1990).
19. Han S.G. et al. *Phys. Rev. Lett.*, **65**, 2708 (1990).
20. Gershenzon M.E. et al. *Pis'ma Zh. Eksp. Teor. Fiz.*, **52**, 1189 (1990).
21. Kazeroonian A.S. et al. *Solid State Commun.*, **78**, 95 (1991).
22. Chekalin S.V. et al. *Phys. Rev. Lett.*, **67**, 3860 (1991).
23. Bluzer N. *Phys. Rev. B*, **44**, 10222 (1991).
24. Hegman F.A. et al. *Appl. Phys. Lett.*, **62**, 1158 (1993).
25. Zherikhin A.N. et al. *Physica C*, **221**, 311 (1994).
26. Zherikhin A.N. et al. *Kvantovaya Elektron.*, **21**, 574 (1994) [*Quantum Electron.*, **24**, 529 (1994)].
27. Brorson S.D. et al. *Phys. Rev. B*, **49**, 6185 (1994).
28. Buhleier R. et al. *Phys. Rev. B*, **50**, 9672 (1994).
29. White J.O. et al. *Physica C*, **235-240**, 2025 (1994).
30. Stevens C.J. et al. *Phys. Rev. Lett.*, **78**, 2212 (1997).
31. Smith D.C. et al. *J. Low Temp. Phys.*, **117**, 1059 (1999).
32. Demsar J. et al. *Phys. Rev. B*, **63**, 054519 (2001).
33. Segre G.P. et al. *Phys. Rev. Lett.*, **88**, 137001 (2002).
34. Schneider M.L. et al. *Eur. Phys. J. B*, **36**, 327 (2003).
35. Bobyrev Yu.V. et al. *Kvantovaya Elektron.*, **33**, 998 (2003) [*Quantum Electron.*, **33**, 998 (2003)].
36. Voronov A.V. et al. *Kvantovaya Elektron.*, **31**, 1058 (2001) [*Quantum Electron.*, **31**, 1058 (2001)].
37. Bobyrev Yu.V. et al. *Kvantovaya Elektron.*, **31**, 1067 (2001) [*Quantum Electron.*, **31**, 1067 (2001)].
38. Allen P.B. *Phys. Rev. Lett.*, **59**, 1460 (1987).
39. Nessler W. et al. *Phys. Rev. Lett.*, **81**, 4480 (1998).
40. Sun C.K. et al. *Phys. Rev. B*, **50**, 15337 (1994).

41. Demsar J. *cond-mat/0305597* (2003).
42. Kaganov M.I. et al. *Zh. Eksp. Teor. Fiz.*, **31**, 242 (1956).
43. Haberland P.H., Shiffman C.A. *Phys. Rev. Lett.*, **19**, 1337 (1967).
44. Gantmakher V.F., Leonov Yu.S. *Pis'ma Zh. Eksp. Teor. Fiz.*, **8**, 264 (1968).
45. Bradfield J.E., Coon J.B. *Phys. Rev. B*, **7**, 5072 (1973).
46. Tinkham M., Clarke J. *Phys. Rev. Lett.*, **28**, 1366 (1972).
47. Kabanov V.V. et al. *Phys. Rev. B*, **61**, 1477 (2000).
48. Farztdinov V.M. et al. *Brazilian J. Phys.*, **26**, 482 (1996).
49. Lucas G., Stephen M.J. *Phys. Rev.*, **154**, 349 (1967).
50. Woo J.W.F., Abrahams E. *Phys. Rev.*, **169**, 407 (1968).
51. Schmid A., Schoen G. *J. Low Temp. Phys.*, **20**, 207 (1975).
52. Demsar J. et al. *Phys. Rev. Lett.*, **82**, 4918 (1999).
53. Schneider M.L. et al. *Europhys. Lett.*, **60**, 460 (2002).
54. Bonn D.A. et al. *Phys. Rev. B*, **47**, 11314 (1993).
55. Quinlan S.M. et al. *Phys. Rev. B*, **49**, 1470 (1994).
56. Voronov A.V. et al. *Zh. Eksp. Teor. Fiz.*, **120**, 1256 (2001).
57. Abakumov V.N. et al. *Bezyzluchatel'naya rekombinatsiya v poluprovodnikakh* (Nonradiative Recombination in Semiconductors) (St. Petersburg: Izd. B.P. Konstantinov St. Petersburg Institute of Nuclear Physics, RAS, 1997).
58. Animalu A. *Kantovaya teoriys kristallicheskikh tverdykh tel* (Quantum Theory of Crystalline Solids) (Moscow: Mir, 1981).
59. Perry J.K. et al. *Phys. Rev. B*, **63**, 144501 (2001).
60. Kornienko A.G. et al. *J. Appl. Phys.*, **80**, 2396 (1996).
61. Bobyrev Yu.V. et al. *Kvantovaya Elektron.*, **35**, 102 (2005) [*Quantum Electron.*, **35**, 102 (2005)].
62. Chadi D.J., Cohen M.L. *Phys. Rev. B*, **8**, 5747 (1973).
63. Koroteev N.I. *Vestn. Mosk. Univ., Ser. Fiz. Astron.*, no. 6, 6 (1996).